

# Adaptive Silver Films for Detection of Antibody–Antigen Binding

Vladimir P. Drachev,<sup>\*,†</sup> Vishal C. Nashine,<sup>‡</sup> Mark D. Thoreson,<sup>†</sup> Dor Ben-Amotz,<sup>§</sup>  
V. Jo Davisson,<sup>‡</sup> and Vladimir M. Shalaev<sup>†</sup>

*School of Electrical and Computer Engineering, Department of Medicinal Chemistry  
and Molecular Pharmacology, and Department of Chemistry, Purdue University,  
West Lafayette, Indiana 47907*

*Received January 27, 2005. In Final Form: June 21, 2005*

Antibody–antigen binding events at a monolayer protein concentration have been demonstrated on nanostructured adaptive silver films (ASFs) using surface-enhanced Raman scattering (SERS) and luminescence-based assays. It is shown that proteins stabilize and restructure the ASF to increase the SERS signal while preserving antigen-binding activity. Evidence for antibody–antigen binding on the ASF substrates is the distinct SERS spectral changes of the surface-bound antibody or antigen without special tags. The activity of the surface-bound proteins and their practical application are validated by independent immunochemical assays. Results are presented to demonstrate that these surfaces can be extended to protein arrays with detection applications distinct from current SERS, fluorescence, or luminescence methods.

## Introduction

The detection of protein binding by optical means is of critical importance to current protein analysis, and promises to lead to a number of exciting future applications in biomedical diagnostics, research, and discovery. Detection of protein–ligand binding events most commonly involves labeling strategies with a variety of schemes including scintillation counting,<sup>1</sup> electrochemical changes,<sup>2</sup> enzymatic transformation,<sup>3</sup> fluorescence,<sup>4,5</sup> chemiluminescence,<sup>6</sup> or quantum dots.<sup>7</sup> More recent advances involve the use of surface plasmon resonance (SPR)<sup>8–10</sup> or surface-enhanced Raman scattering (SERS).<sup>11–13</sup> One of the SERS-based approaches takes advantage of the binding properties of antibody and antigen molecules (or DNA strands) and uses metal nanoparticles coated with Raman-

active chromophores as tags.<sup>14–17</sup> To provide the needed level of enhancement, silver clusters are added to form a complex sandwich structure that includes a nanoparticle labeled with the Raman-active dye, complementary biomolecules, and the metal clusters. This method relies on chromophores which produce SERS (also called SERRS). SERRS spectra of dye labels are detected, rather than the spectra of the complementary biomolecules (proteins or DNA). The SPR sensing technique<sup>8–10</sup> does not require an external label for detection, and the sensitivity can be increased with shaped nanoparticles.<sup>14</sup> In this approach, antigen binding produces a small spectral shift in the SPR for a metal nanoparticle coated with antibodies. The spectral shift occurs because the formation of the antigen–antibody complex results in a change in the refractive index for the dielectric coating formed by the proteins on the nanostructured metal surface. Thus, in the SPR approach one measures the spectrum of a metal surface plasmon and detects its modifications induced by protein binding.

Label-free, direct detection of an antigen–antibody complex by the SERS signal from protein has been reported.<sup>18</sup> This near-infrared SERS-based approach involved the use of colloidal gold to detect the antigen–antibody complex formation, without separation of free antigen or antibody. Widespread use of this technique has probably been hindered because the solution-phase SERS spectrum of the antigen-bound antibody would, in the absence of purification or separation steps, likely be affected by the composition and amounts of other proteins and salts in the solution. Other reported applications of SERS for label-free detection of specific protein–ligand

\* To whom correspondence should be addressed. E-mail: vdrachev@ecn.purdue.edu.

<sup>†</sup> School of Electrical and Computer Engineering.

<sup>‡</sup> Department of Medicinal Chemistry and Molecular Pharmacology.

<sup>§</sup> Department of Chemistry.

(1) Gutcho, S.; Mansbach, L. *Clin. Chem.* **1977**, *23*, 1609.

(2) Hayes, F. J.; Halsall, H. B.; Heineman, W. R. *Anal. Chem.* **1994**, *66*, 1860.

(3) Butler, J. E. *J. Immunoassay* **2000**, *21*, 165.

(4) Vuori, J.; Rasi S.; Takala T.; Vaananen K. *Clin. Chem.* **1991**, *37*, 2087.

(5) Xu, Y. Y.; Pettersson, K.; Blomberg, K.; Hemmila, I.; Mikola, H.; Lovgren, T. *Clin. Chem.* **1992**, *38*, 2038.

(6) Brown, C. R.; Higgins, K. W.; Frazer, K.; Schoelz, L. K.; Dyminski, J. W.; Marinkovich, V. A.; Miller, S. P.; Burd, J. F. *Clin. Chem.* **1985**, *31*, 1500.

(7) Chan, W. C. W.; Nie, S. *Science* **1998**, *281*, 2016.

(8) Lyon, L. A.; Musik, M. D.; Natan, M. J. *J. Anal. Chem.* **1998**, *70*, 5177.

(9) Knoll, W.; Zizlsperger, M.; Liebermann, T.; Arnold, S.; Badia, A.; Liley, M.; Piscevic, D.; Schmitt, F. J.; Spinke, J., *J. Colloids Surf., A* **2000**, *161*, 115.

(10) Nelson, B. P.; Grimsrud, T. E.; Liles, M. R.; Goodman, R. M.; Corn, R. M. *Anal. Chem.* **2001**, *73*, 1.

(11) Rorh, T. E.; Cotton, T.; Fan, N.; Tarcha, P. J. *J. Anal. Biochem.* **1989**, *182*, 388.

(12) Dou, X.; Takama, T.; Yamaguchi, Y.; Yamamoto, H.; Ozaki, Y. *Anal. Chem.* **1997**, *69*, 1492.

(13) Ni, J.; Lipert, R. J.; Dawson, G. B.; Porter, M. D. *Anal. Chem.* **1999**, *71*, 4903.

(14) Riboh, J. C.; Haes, A. J.; MacFarland, A. D.; Yonzon, C. R.; Van Duyne, R. P. *J. Phys. Chem. B* **2003**, *107*, 1772.

(15) Cao, Y. W. C.; Jin, R.; Mirkin, C. A. *Science* **2002**, *297*, 1536.

(16) Charles, C. Y.; Jin, R.; Thaxton, C. S.; Mirkin, C. A. *J. Am. Chem. Soc.* **2003**, *125*, 14676.

(17) Vo-Dinh, T.; Stokes, D. L. In *Biomedical Photonics Handbook*; Vo-Dinh, T., Ed.; CRC Press LLC: Boca Raton, FL, 2003; pp 64.1–64.39.

(18) Dou, X.; Yamaguchi, Y.; Yamamoto, H.; Doi, S.; Ozaki, Y. *J. Raman Spectrosc.* **1998**, *29*, 739.

interactions include binding of aflatoxins to RNA polymerase and microorganisms to cognate antibodies.<sup>19</sup>

A substrate based on adaptive silver nanostructures has been recently described which allows SERS spectra of proteins to be obtained at monolayer surface density.<sup>20</sup> The adaptive property of this substrate enables the adsorption of proteins without significant alteration in their conformational state. The evidence from the SERS spectra of human insulin and insulin lispro reveals features unique to different conformational states, which is in agreement with X-ray crystallographic studies.<sup>20</sup>

In this paper we demonstrate that SERS substrates based on nanostructured adaptive silver films (ASFs) make it possible to detect the formation of specific antigen–antibody complexes at a monolayer level by SERS, fluorescence, and chemiluminescence techniques. As we will show, the antibodies rearrange and stabilize the silver film to make the complex resistant to washing and incubation procedures while preserving their activity as recognition agents. The ASF substrates can potentially be used for routine laboratory analyses in ways similar to those of membrane-based immunoblotting protocols. One advantage of the ASF substrate is that it does not require chromophore-tagged secondary antibodies since direct detection of SERS spectral signatures associated with the antigen–antibody binding event are observed. These early-stage demonstrations illustrate opportunities for the use of nanoparticle surface systems for analysis of biomolecular interactions relevant for diagnostic applications.

## Materials and Methods

**Materials.** The anti-FLAG M2 monoclonal antibody (fAb), bacterial alkaline phosphatase/C-terminal FLAG-peptide fusion (fBAP), Cy3 dye-conjugated monoclonal anti-FLAG antibody (Cy3–fAb), and horseradish peroxidase (HRP)-conjugated anti-mouse IgG used in these experiments were obtained from Sigma-Aldrich. Bacterial alkaline phosphatase (BAP) without the FLAG peptide was generated by enterokinase-catalyzed cleavage of FLAG peptide. fBAP protein was diluted to a concentration of 500 ng/mL in dilution buffer (10 mM Tris–HCl, 10 mM CaCl<sub>2</sub>, pH 8.0), and 20 U of enterokinase was added followed by incubation at 37 °C for 24 h. The completion of the reaction was followed by slot-blot (Schleicher and Schuell) on a nitrocellulose membrane. The free peptide was removed using the Ultrafree0.5 (5000 MWCO) spin concentrators (Millipore). Water used in these studies was obtained from Burdick and Jackson.

**Preparation of Adaptive Silver Films.** Fabrication of a nanostructured ASF involves the deposition of thin films on a dielectric substrate under vacuum evaporation with an electron beam. Microscope glass slides (from Fisher) were cut into 2.5 cm × 2.5 cm sections for use as initial substrates. The cut slides were cleaned through several steps, including multiple solvent rinses, a piranha (H<sub>2</sub>O<sub>2</sub>/3H<sub>2</sub>SO<sub>4</sub>) acid bath, rinsing in 18 MΩ deionized water, and drying with pressurized gaseous nitrogen. Silver shot from Alfa Aesar (99.9999%, 1–3 mm) and SiO<sub>2</sub> pellets from Lesker (99.995%, cut quartz) were used for fabrication of the ASFs on the glass substrates. The thin film deposition was performed in a modified Varian electron beam evaporator with an initial pressure inside the system of approximately 10<sup>−7</sup> Torr. The film thickness and deposition rate were monitored with a quartz crystal oscillator. The glass sections were covered first by a sublayer of SiO<sub>2</sub> (10 nm) followed by a Ag layer (10–13 nm) deposited at a rate of 0.05 nm/s. The fabricated films were characterized by field emission scanning electron microscopy (FESEM), atomic force microscopy (AFM), and a Lambda 35 spectrophotometer (Perkin-Elmer) equipped with a Labsphere. High-resolution FESEM images were obtained through MAS,

Inc. (Raleigh, NC). AFM images (not shown here) were acquired with a Dimension 3100 (DI Veeco) using a 10 nm Si tip for measuring the height profiles of our samples.

**Methods. Protein Deposition and Immunoreactions.** The protocols followed in the experiments were similar to the Western blotting procedure provided by Sigma. Aliquots (2 μL) of 0.5 μM solutions of fBAP and/or BAP were manually deposited on the ASF substrate and incubated for 2 h under shaking conditions at room temperature. The substrates were then rinsed with Tris-buffered saline (TBS; consisting of 50 mM Tris, HCl (pH 8.0), 0.138 M NaCl, and 2.7 mM KCl) and probed with fAb in TBS buffer. The excess fAb was rinsed with TBS followed by washing with water. Spectra were collected as described below. In the case of the reverse experiment, the antibody (fAb) was deposited on the surface and probed with fBAP or BAP.

**Acquisition of SERS Spectra.** Spectra were collected at a laser wavelength of 568 nm, 1 mW power, and an exposure time of 200 s and were subjected to background subtraction using a Fourier method. The specific intensities for fAb and fBAP SERS signals were about 4–7 counts/smW measured at the 1000 cm<sup>−1</sup> peak. SERS spectra were collected and compared after each washing step to observe any differences caused by a binding (or loss) event. A four-wavelength Raman system was used, which consists of an Ar/Kr ion laser (Melles Griot), a laser band-path holographic filter (to reject plasma lines), two Super-Notch Plus filters to reject Rayleigh scattering (Kaiser Optical Systems), focusing and collection lenses, an Acton Research 300i monochromator with a grating of 1200 grooves/mm, and a nitrogen-cooled CCD (1340 × 400 pixels, Roper Scientific). An objective lens (f/1.6) provided a collection area of about 180 μm<sup>2</sup>. Collected light was delivered to the monochromator via a fiber bundle. The spectral resolution was about 3 cm<sup>−1</sup> with a laser power of approximately 1 mW and an exposure time of 100–200 s.

**Chemiluminescence and Fluorescence Detection.** In the chemiluminescence experiment, the formation of the antigen–antibody complex was followed by incubation with HRP-conjugated secondary antibody. After removal of excess reagent and washing with TBS, the formation of luminescent product was detected using a CCD camera (Alpha Innotech) upon incubation with luminol. For the fluorescence detection, antigen was probed using Cy3–fAb (instead of fAb) and imaged on Typhoon 8600 (GE Healthcare). The chemiluminescence and fluorescence data were processed using ImageQuant TL. In the microarray experiment, 1–100 nL of a 0.5 μM solution of fAb was spotted on an ASF substrate, blocked with TBS containing 3% milk, and reacted with HRP-conjugated secondary antibody.

## Results and Discussion

**Adaptive Silver Films.** Metal films have been used for SERS studies for more than 25 years.<sup>17,21–25</sup> Their physical and optical properties depend on evaporation parameters, mass thickness, and the material in the sublayer(s). The capability of the silver films used in these studies for bioassay applications is initiated by the deposition of the protein. In our recent work, silver films fabricated at a certain range of evaporation parameters allow fine rearrangement of the nanostructure upon protein deposition.<sup>20</sup> This restructuring forms cavity sites enclosed by two or more metal particles, which are typically optimal for SERS. In this case, these cavity sites are naturally filled with the protein molecules. Because of these features, a nanostructured evaporated film that allows restructuring is herein referred to as *adaptive*. Previous experiments with ASFs show that SERS spectral differences attributed to the distinct conformational states of human insulin and its analogue, insulin lispro, can be

(19) Chen, C. Y.; Burstein, E.; Lundquist, S. *Solid State Commun.* **1979**, *32*, 63.

(20) Pockrand, I.; Otto, A. *Solid State Commun.* **1980**, *35*, 861.

(21) Bergman, J. G.; Chemla, D. S.; Liao, P. F.; Glass, A. M.; Pinczuk, A.; Hart, R. M.; Olson, D. H. *Opt. Lett.* **1981**, *6*, 33.

(22) Weitz, D. A.; Garoff, S.; Gramila, T. J. *Opt. Lett.* **1982**, *7*, 168.

(23) Li, X.; Xu, W.; Zhang, J.; Jia, H.; Yang, B.; Zhao, B.; Li, B.; Ozaki, Y. *Langmuir* **2004**, *20*, 1298.

(19) Grow, A. E.; Wood, L. L.; Claycomb, J. L.; Thomson, P. A. *J. Microbiol. Methods* **2003**, *53*, 221.

(20) Drachev, V. P.; Thoreson, M. D.; Khaliullin, E. N.; Davisson, V. J.; Shalae, V. M. *J. Phys. Chem. B* **2004**, *108*, 18046–18052.



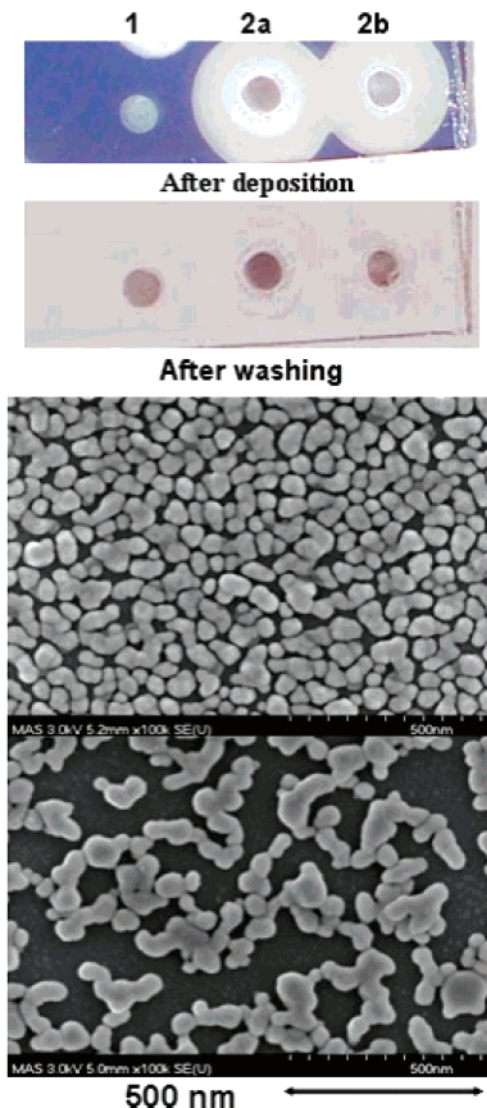


**Figure 1.** ASF film with three protein spots after (top) and subsequent washing (second from the top). Protein spot 1 is from protein in water, and spots 2a and 2b are from protein in buffer. FE SEM images of the ASF (11 nm mass thickness) before (second from the bottom) and after protein deposition and washing (bottom).

observed at submonolayer coverage of protein molecules.<sup>20</sup> The measured macroscopic enhancement factor for these ASFs is about  $3 \times 10^6$ , which is among the largest observed for random metal-dielectric films.

Figure 1 shows a representative ASF image and its nanostructure before and after antibody deposition. After the film is washed with TBS/Tween-20, the nonadherent metal is removed from the substrate except in the areas where protein (antibody) has been deposited. Stabilization of the ASF by the proteins was not altered by the presence of buffer in the solution, as shown in Figure 1, underscoring the key role of proteins in forming a stable complex with the substrate metal particles. At low concentrations of protein, no silver particles are left in the deposition area and absorption is very low. In this case, the silver metal reacts with chlorine ions in the buffer solution to form AgCl crystals on the substrate surface, which was confirmed by X-ray diffraction. Absorbance inside a deposition area is linearly dependent on the protein concentration, which also confirms the stabilization of the silver film by proteins. The protein-mediated restructuring, illustrated by FESEM images in Figure 1, results in

the formation of aggregates of closely spaced silver particles covered with proteins, as opposed to the relatively dispersed particles of the initial film before protein deposition. Depending on the mass thickness of the initial film, small or large fractal-like aggregates can be formed. The small aggregates are not shown here, but are similar to those shown for insulin.<sup>20</sup> The large aggregates are shown in the bottom image in Figure 1. The protein SERS signal, normalized per metal mass coverage, is comparable for all of the types of protein-adapted aggregates (small and large) that were examined. As shown below, SERS enhancement is high enough to detect a monolayer of antibody or antigen and is similar to the case for insulin.<sup>20</sup>

The interest in developing new SERS surfaces is driven by the promise that they hold in developing novel SERS applications. Nanostructured metal films of gold or silver colloids suitable for SERS have been described previously. In some of these reports, silver nanoparticles were self-assembled on glass slides by a chemical reaction,<sup>25–27</sup> and in one instance, thin film islands of silver nanoparticles were formed by depositing drops of silver colloid/analyte mixtures on a glass slide and allowing the water to evaporate.<sup>28</sup> In all these instances, it is not clear if these substrates can be washed extensively before the acquisition of the spectra. The ability to retain analytes on the surface through several washing steps is a valuable attribute for surfaces that are targeted for analyses of complex biological materials, where removal of interfering compounds greatly increases sensitivity and specificity.

The aggregated structures reveal conditions for both electromagnetic and chemical SERS enhancements. Even the small aggregates provide strong electromagnetic enhancement in the visible and near-infrared, as has been shown for polarization nonlinearities<sup>29</sup> and SERS.<sup>30</sup> Large aggregates typically have a fractal morphology, which is known to provide particularly strong SERS.<sup>31,32</sup> The effects of the first molecular layer also involve closely spaced metal particles that make an optical tunnel current possible, either through the molecule at the point of nearest approach between two metal particles<sup>33</sup> or through a system operating as a molecular tunnel junction between particles across a vibrating molecular bridge.<sup>34</sup> Thus, ASFs are ideally suited for SERS sensing of proteins because proteins not only stabilize the films but also improve SERS.

**Label-Free SERS Detection.** To probe the antigen–antibody binding event using SERS, a general protocol was devised that involves first the deposition and immobilization of a monoclonal antibody or a corresponding antigen on an ASF substrate. Typically, 2  $\mu$ L of 0.5  $\mu$ M Ab solution forms a spot of about 2 mm after drying overnight, similar to that shown in Figure 1. The non-

(26) Zhang, J.; Li, X.; Liu, K.; Cui, Z.; Zhang, G.; Zhao, B.; Yang, B. *J. Colloid Interface Sci.* **2002**, *255*, 115.

(27) Li, X.; Xu, W.; Jia, H.; Wang, X.; Zhao, B.; Li, B.; Ozaki, Y. *Appl. Spectrosc.* **2004**, *58*, 26.

(28) Hu, J.; Zhao, B.; Xu, W.; Fan, Y.; Li, B.; Ozaki, Y. *Langmuir* **2002**, *18*, 6839.

(29) Drachev V. P., Perminov S. V., Rautian S. G., and Safonov V. P. In *Optical Properties of Nanostructured Random Media*; Shalaev, V. M., Ed.; Topics in Applied Physics Series, Vol. 82; Springer-Verlag: Berlin, 2001; pp 113–148.

(30) Kneipp, K.; Wang, Y.; Kneipp, H.; Perelman, L. T.; Itzkan, I.; Dasari, R. R.; Feld, M. *Phys. Rev. Lett.* **1997**, *78*, 1667.

(31) Stockman, M. I.; Shalaev, V. M.; Moskovits, M.; Botet, R.; George, T. F. *Phys. Rev. B* **1992**, *46*, 2821.

(32) Shalaev, V. M. *Nonlinear Optics of Random Media: Fractal Composites and Metal-Dielectric Films*; STMP, Vol. 158; Springer: Heidelberg, 2000.

(33) Holzapfel, S.; Akemann, W.; Schumacher, D.; Otto, A. *Surf. Sci.* **1990**, *227*, 123.

(34) Michaels, A. M.; Jiang, J. J.; Brus, L. E. *J. Phys. Chem. B* **2000**, *104*, 11965.

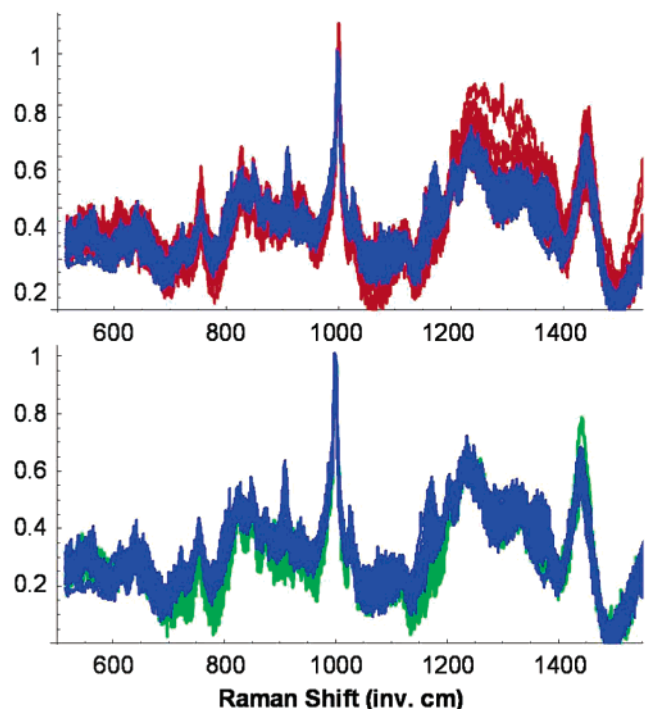


**Figure 2.** SERS spectra of an ASF modified with fAb (blue), the same fAb surface incubated with fBAP (red), and the fAb surface incubated with BAP (green). Each trace presents 15 spectra collected from 3 different positions in 5 different spots.

adherent metal particles were then removed by washing with buffered solution and deionized water to reveal immobilized protein-adapted aggregates representing antibody (or antigen) in a small array. The specific proteins used in our studies include fAb and fBAP. Proteins for control experiments included BAP without the FLAG peptide that was generated by enterokinase cleavage. Subsequent incubation of the protein-adapted aggregates with antigen (or antibody) was conducted, and the nonspecifically bound material was removed by washing with a standard buffer solution for Western blotting (TBS/Tween-20) followed by rinsing five times with deionized water (the Western blot procedure was provided by Sigma). SERS spectra of the immobilized fAb (or fBAP) were compared before and after reaction with the cognate antigen (or antibody) partner.

An estimation of the protein coverage on the ASF substrates is based on the protein concentration and the density of the average deposition area defined by a central cluster and an outer ring. The area of the central part and the area of the ring are both typically about  $4 \text{ nm}^2$ . For a protein concentration of  $0.5 \mu\text{M}$  and a deposition volume of  $2 \mu\text{L}$ , an average protein density of  $D_{\text{av}} = 120 \text{ fmol}/\text{mm}^2$  or  $0.072 \text{ molecules}/\text{nm}^2$  can be estimated. If a single protein molecule occupies an average area of approximately  $20 \text{ nm}^2$ , then 1.4 layers of protein would be expected in each cluster. This value would represent an upper limit since any loss of protein during the washing steps would reduce the surface coverage. Therefore, we infer that all of the above experiments were performed at approximately monolayer or submonolayer coverage conditions.

The immobilized fAb/metal clusters yielded reproducible SERS results, and representative spectra are shown in Figure 2. Upon incubation with fBAP ( $1 \text{ nM}$ ), spectral changes were observed, with the most dominant features appearing in the  $1200\text{--}1400 \text{ cm}^{-1}$  region. To establish the specificity of the spectral changes, two fAb arrays on similar SERS substrates were probed with different

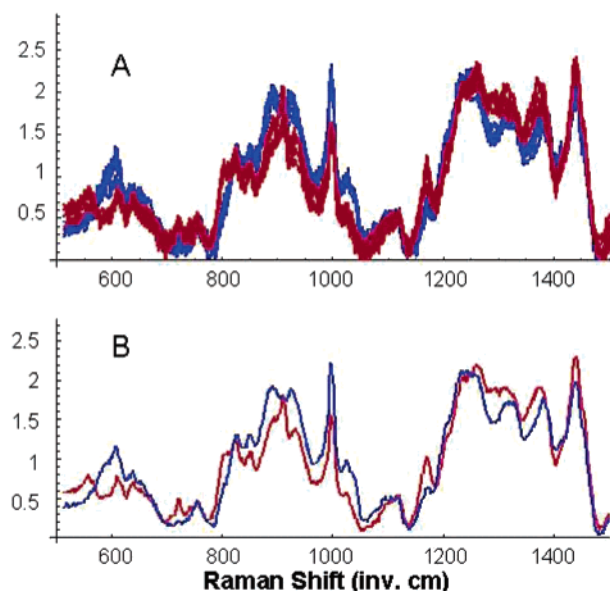


**Figure 3.** SERS spectra of fBAP on the ASF substrate (blue) and the same fBAP-modified surface after incubation with fAb solution (red): (A) nine spectra, each obtained from three spots; (B) average of the nine spectra.

proteins. One array was incubated with fBAP at a concentration of  $0.75 \text{ nM}$  in TBS, while the second array was probed with BAP at a concentration of  $0.67 \text{ nM}$  as a control experiment. Fifteen SERS spectra were collected over five spots for each substrate (three different positions in each metal/protein cluster). Figure 2 shows the superposition of multiple spectra on both substrates. The spectra of the fAb were consistently altered after incubation with fBAP, but remained unchanged after incubation with BAP. This is indicative of a specific antibody–antigen binding event, with the most pronounced changes in the  $1200\text{--}1400 \text{ cm}^{-1}$  region. The spectral variation is attributed to a spatial variation in the distribution of antigen binding. The fAb/metal clusters derived from multiple ASF surfaces revealed reproducible SERS spectra, and in all cases, the formation of specific antibody–antigen complexes resulted in the same characteristic spectral change in the  $1200\text{--}1400 \text{ cm}^{-1}$  region.

To further validate our observations regarding the specific interactions on the protein-adapted aggregates, fBAP was first deposited on an SERS substrate followed by fAb incubation. Specifically, three  $2 \mu\text{L}$  aliquots of fBAP at  $0.5 \mu\text{M}$  in TBS buffer were deposited on the substrate, dried overnight, and then incubated with fAb at a concentration of about  $4 \text{ nM}$ .

The results of the SERS measurements are shown in Figure 3, and the spectra of fBAP/metal clusters undergo changes after incubation with the fAb solution. These changes are most evident in the group of peaks centered at  $900 \text{ cm}^{-1}$ , where a triple peak appears instead of the double peak present before incubation with antibody. The intensity of the peak at  $1000 \text{ cm}^{-1}$  is also significantly decreased, while that around  $1280 \text{ cm}^{-1}$  is increased.

For both the experiments, the signal from the first layer of protein dominates the SERS spectra observed from the immune complex. Therefore, the spectra shown in Figures 2 and 3 are significantly different, with the former being primarily the SERS spectrum of fAb and the latter representing the fBAP spectrum. In both cases, binding with proteins of the second layer results in detectable and reproducible changes in the SERS spectrum of the first layer. The fact that the first layer dominates the observed



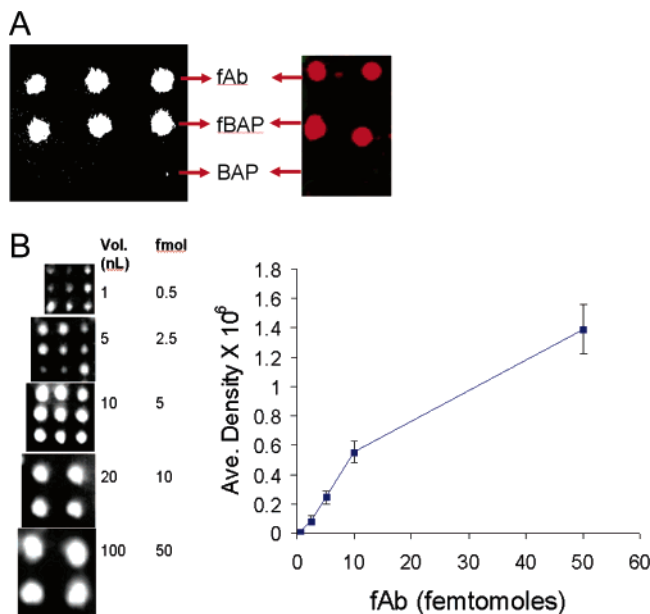


**Figure 4.** (A) Chemiluminescence (left) and fluorescence (right) detection on the ASF substrate. The labels indicate proteins that were deposited on the ASF. In the chemiluminescence case, the deposited proteins were probed with fAb followed by HRP-tagged secondary antibody. For the fluorescence experiment (right), the label “fAb” refers to Cy3–fAb. The deposited proteins were probed with Cy3–fAb. (B) Quantification of the chemiluminescence signal in array format. Here, fAb deposited on the ASF was probed with HRP-tagged secondary antibody.

SERS spectra indicates the important role of surface chemical enhancement, which is multiplied by the electromagnetic enhancement.

**Chemiluminescence and Fluorescence Detection with ASF Substrates.** Alternative detection methods were used to validate the integrity of the fAb–fBAP binding events on the ASF substrate and to assess the utility of the protein-adapted clusters for applications in protein binding assays. The protein-adapted silver clusters as described above were also used directly with fluorescence or chemiluminescence detection strategies. For detection by chemiluminescence, fAb, fBAP, and BAP were each deposited on an ASF substrate at equal concentrations and sequentially reacted with fAb and HRP-conjugated anti-mouse IgG secondary antibody. The specificity of the reactions shown in Figure 4A indicates that fAb and the secondary antibody are functional on these adapted surfaces in both the first and second layers. Similar experiments were performed for fluorescence detection except that the Cy3-conjugated fAb, fBAP, and BAP were arrayed and probed with Cy3-conjugated fAb (Figure 4A). As anticipated, the specific interaction of the Cy3-conjugated fAb is observed with the fBAP, and the fluorescence is observed for both the first and second layers of the protein-adapted silver clusters. These results are consistent with those observed using the secondary antibody/chemiluminescence detection strategy. In both cases, the results indicate that the functional properties of immobilized proteins are largely preserved on the ASF substrate. Moreover, Figure SF1 (see the Supporting Information) indicates that ASF surfaces can be adapted for multiplexed analysis with a variety of antigen–antibody pairs.

To evaluate the compatibility of the ASF as a protein array substrate for high-throughput analysis, a series of nanoliter volumes of the fAb solution were deposited on the ASF surface with a microdrop dispenser. A washing

procedure was used to reveal islands of protein-adapted silver clusters of differing sizes (Figure 4B). Detection of the fAb was accomplished using HRP-conjugated anti-mouse IgG secondary antibody followed by incubation with H<sub>2</sub>O<sub>2</sub>/luminol and imaging with a CCD camera. As expected, the signal intensity was centered on the areas of the protein/metal clusters. At the densities created using this simple protocol, detection of the secondary antibody binding was achieved at a 0.5 fmol level. Integration of the signals due to chemiluminescence enabled an estimate of the linearity of the response, and the data presented indicate potential for optimization.

The application of these ASF materials for protein detection using established optical methods such as fluorescence and chemiluminescence methods have potential given the adaptive features of these planar surfaces. The protein dependence of the adapted aggregates may provide some added capabilities of the ASF substrates to preserve the physicochemical properties of the protein and enhance the capacity to retain functionality. Orientation of the protein with respect to the surface does not require a covalent linkage and can potentially preserve the tertiary structure of the deposited protein.<sup>35,36</sup> In a similar way, these surfaces coupled with sensitive detection strategies could prove advantageous over typical membrane-based protein blotting methods since the irregular features of the membrane will not render a population of protein inaccessible. Although the sensitivity and dynamic range of immunoassays performed on ASFs need to be optimized before comparison with commercially available substrates, our preliminary results with chemiluminescence detection show that the detection limit will probably be comparable.<sup>36,37</sup> Both the first and second layers of protein adsorbed to the silver nanoparticles are SERS-active, suggesting that these surfaces are amenable for analyses of interactions of protein with low molecular weight ligands as well. Finally, the preservation of biological activity in the protein/metal clusters implies the potential application of ASF substrates for conformationally demanding systems such as enzymes.<sup>38</sup>

## Conclusion

Adaptive nanostructures formed through the aggregation of proteins and silver films offer several opportunities for the creation of planar surface arrays. A central feature of this approach is the stabilization of the ASF by the protein-mediated clustering event, which does not require covalent attachment of the protein to the surface. No additional steps or equipment are necessary to separate samples on a substrate. These ASF substrates offer several advantages over previously described SERS substrates for analyses of protein–ligand interactions. To date, the results are consistent with a property that proteins optimize the local nanostructure in such a way that conditions for SERS are improved and, in parallel, proteins may experience *soft* adsorption, preserving their binding ability. We show that SERS substrates based on ASFs can be used for direct, sensitive, and label-free detection of protein binding at a monolayer level. Because the silver particles are washed away in areas where the particles are not stabilized by protein, the background due to

(35) Nam, J. M.; Han, S. W.; Lee, K. B.; Liu, X.; Ratner, M. A.; Mirkin, C. A. *Angew Chem., Int. Ed.* **2004**, *43*, 1246.

(36) Angenendt, P.; Glokler, J.; Sobek, J.; Lehrach, H.; Cahill, D. J. *J. Chromatogr., A* **2003**, *1009*, 97.

(37) Angenendt, P.; Glokler, J.; Murphy, D.; Lehrach, H.; Cahill, D. J. *J. Anal. Biochem.* **2002**, *309*, 253.

(38) Houseman, B. T.; Huh, J. H.; Kron, S. J.; Mrksich, M. *Nat. Biotechnol.* **2002**, *20*, 270–274.

nonspecific protein–ligand interactions is expected to be low. The results described in this paper show that the ASF substrates are useful when applied in standard immunoblotting experiments with common laboratory equipment and fluorescence, chemiluminescence, or SERS detection. When considered with all the other attributes of these surfaces, the ability to perform analyses on a monolayer scale indicates that ASF substrates have potential for high-throughput analyses of protein–ligand interactions with or without tags. Novel, practical uses of these ASF substrates for protein analyses await further systematic studies of the properties of these ASF substrates.

**Acknowledgment.** We thank E. Khaliullin for his assistance with spectrum treatment and Dr. Dongmao Zhang and Dr. Meena Narasimhan for help with microdeposition and helpful discussions that led to this paper. This work was supported by a grant from Inproteo LLC as well as NSF Grant HRD-0317722 and NASA Grant NCC-31035.

**Supporting Information Available:** Figure showing fluorescence-based multiplexing on an ASF substrate. This material is available free of charge via the Internet at <http://pubs.acs.org>.

LA0502490